# Development of GROMOS-Compatible Parameter Set for Simulations of Chalcones and Flavonoids

Pablo R. Arantes,[†] Marcelo D. Polêto,[†] Elisa B. O. John,[†] Conrado Pedebos,[†,‡,¶] Bruno I. Grisci,[§] Marcio Dorn,[§] and Hugo Verli*[,†]

[†]*Centro de Biotecnologia, Universidade Federal do Rio Grande do Sul, Porto Alegre, RS, Brazil*

[‡]*School of Pharmacy, University of Nottingham, University Park, Nottingham, U.K.*

[¶]*CAPES Foundation, Ministry of Education of Brazil, BrasÃηlia, Brazil.*

[§]*Instituto de Informática, Universidade Federal do Rio Grande do Sul, Porto Alegre, RS, Brazil*

E-mail: hverli@cbiot.ufrgs.br

Phone: +55 (51) 3308-7770. Fax: +55 (51) 3308-7309

**Abstract**

Chalcones and flavonoids constitute a large family of plant secondary metabolites that has been explored as a potential source of novel pharmaceutical products. While the simulation of these compounds by molecular dynamics (MD) can be a valuable strategy to assess their conformational properties and so further develop their role in drug discovery, there are no set of force field parameters specifically designed and experimentally validated for their conformational description in condensed phase. So the current work developed a new parameter set for MD simulations of these compounds main scaffolds under GROMOS force field. We employed a protocol adjusting the atomic charges and torsional parameters to the respective quantum mechanical derived dipole moments and dihedrals rotational profiles, respectively. Experimental properties of organic liquids were used as references to the calculated values to validate the parameters. Additionally, metadynamics simulations were performed to evaluate the conformational space of complex chalcones and flavonoids, while NOE contacts during simulations were measured and compared to experimental data. Accordingly, the employed protocol allowed us to obtain force field parameters that reproduce well the target data and may be expected to contribute in more accurate computational studies on the biological/therapeutical role of such molecules.

# Introduction

Plant secondary metabolites have been studied for many years as potential novel therapeutic agents,[1,2] possibly inspired by a long history of application of herbal extracts in traditional folk medicine.[2,3] Among them, chalcones and flavonoids consistently have drawn attention mainly because of their extensive range of biological activities, such as cytotoxic,[4–6] antioxidant,[7] chemopreventive,[8] antimicrobial[9] or inhibitory effects against enzymes of medical relevance,[10–12] what makes these molecules appealing for exploration in the medicinal chemistry.

The classical chalcone scaffold is constituted by two phenyl rings united by an $\alpha, \beta$ unsaturated ketone system. The latter chemical signature is believed to play an important role in the biological activity of chalcones, since the unsaturated functional group can act as an acceptor in Michael reactions' and so promptly be modified when interacting with several compounds.[13] Flavonoids are related molecules, derived from chalconoid precursors that undergo cyclization in the $\alpha, \beta$ unsaturated ketone system, resulting in the presence of an heterocyclic ring connecting the other two phenyl rings. Changes in their structures have been proven useful for the development of new therapeutic candidates and, therefore, increasing the pharmaceutical interest for these biomolecules, which have been intensively studied and modified.[14–16]

In such process of lead optimization, computational methods provide insightful information to rationalize, model and predict new chemical entities and their pharmacological properties.[17,18] Among those methods, molecular dynamics (MD) simulations can be used to anticipate, complement or explain experimental data,[19,20] providing detailed conformational distributions as a function of both time and space for the compounds of interest, as well as for their respective target-receptors.[21,22] As simulations are able to offer unique, atomic level information about the dynamical recognition of drugs by biological receptors and the consequent signal transduction, reliable results from MD simulations are dependent on, among other factors, the quality and accuracy of the empirical potential energy functions used in such calculations. Thus, a novel parameter set associated to a certain new compound requires careful calibration[23] in order to reproduce proper energies of interaction and conformational profiles in condensed phase. While parameters for biomacromolecules are widely available, the chemical diversity of synthetic compounds and natural products constitute a real challenge to classic force field (FF) based calculations.

The absence of calibrated parameters for natural products or synthetic compounds has increased the use of automated topology generators throughout atomic level investigation based on MD simulations of ligand-receptor complexes. The accessibility and easiness of such

approach contrast with the promiscuous torsional parameters and atomic partial charges based on *in vacuo* quantum calculations rather than a calibrated set to reproduce energies in condensed phase. In this sense, the GROMOS force field has provided rather good parametrization strategies to calibrate torsional barriers and profiles as well as atomic partial charges of organic molecules in order to reproduce not only condensed phase physicochemical properties, but also the conformational profile of small molecules in solution.[24–26]

In this context, and considering the relevance of chalcones and flavonoids families of molecules as scaffolds for the medicinal chemistry, the current work intends to provide a new parameter set for the simulation of such compounds using classic force field calculations, considering their most common chemical modifications. The GROMOS family of force fields was selected for the parameterization strategy due to its adjustment to reproduce condensed phase properties.[27] Accordingly, the molecular mechanical (MM) torsional profiles were fitted to the quantum mechanical (QM) derived ones. For parameterization of the partial charges, the MM atomic charges were fitted to the QM dipole moments and later on submitted to validation against thermodynamic properties of organic liquids.[25] The original approach of GROMOS is to empirically adjust the atomic partial charges in order to reproduce thermodynamic properties. However, as stated by Riniker,[28] there is "an infinite number of charge distributions, which can reproduce the electrostatic potential (ESP) outside a surface encapsulating all charges", which lead us to use a hybrid approach that both preserves the QM dipole moment direction and reproduce thermodynamic properties. Based on their accuracy, we explored the conformational description of chalcones and flavonoids in aqueous and nonaqueous solutions comparing the obtained sampling to NMR data (NOESY). The characterization of compounds solution conformational ensemble is an important step toward a deeper understanding of the determinants for biological activity of the compounds and, consequently, for a more efficient design of new bioactive molecules. We expect that such parameters will be able to properly describe the conformational distribution of chalcones and flavonoids, a starting point to further studies on the biological role of such molecules at

an atomistic level of detail.

# Results and discussion

## Torsional potentials and force field calibration

There are several drawbacks in using automated topology builders in the simulations of small bioactive compounds.[23] Although ATB server[29] has recently demonstrated reasonable accuracy in predicting free enthalpies of hydration,[30] proper torsional designations are still challenging, since they are based on mathematical descriptors of terms already present on the original force field, rather than based on the chemical environment created by atoms involved on the dihedral.[31] On the other hand, a proper set of atomic partial charges plays an important role in describing accurate inter and intramolecular interactions, which may directly impact in the conformational description of small bioactive compounds in simulations.

Hence, several small molecules resembling fragments of the structure of chalcones, flavonoids and their substituents were selected to act as building blocks for the later assembly of complete compounds. These so-called fragments (molecules **1-9** in Figure S1 and 2) had their topologies built with new atomic charges, empirically adjusted to fit into charge groups, maintaining the molecular polarity, as observed in comparisons of dipole moments from ESP-MP2/6-31* calculations.

The derived atomic charges were validated through comparison to experimental thermodynamic properties of condensed-phase ($\rho$ and $\Delta H_{vap}$), as reported in other works involving the parametrization of molecules for the GROMOS force field[24,32–34] and for force field benchmarking.[24,25,35] Individually, most of the parameterized molecules obtained values in good agreement with the experimental data (Table 1). One particular outlier was fragment **2**, which yielded higher absolute errors despite calibration efforts to reduce it. Our QM calculations revealed a dipole moment of 0.2 debye, which suggests a low charge polarity for fragment **2**. Yet, our MM calculations yielded underestimated values of density and enthalpy

of vaporization, most likely due to the lack of $\pi - \pi$ interactions and resonance effects inherently misrepresented in MM calculations. A similar absence of interactions is expected to influence the description of fragment **8** properties.

**Table 1: Obtained values for thermodynamic properties of the simulated fragments as organic liquids.**

| Fragment | Temp. [K] | Exp. $\rho$ $[g/cm^3]$ | Calc. $\rho$ $[g/cm^3]$ | Error | Exp. $\Delta H_{vap}$ $[kJ/mol]$ | Calc. $\Delta H_{vap}$ $[kJ/mol]$ | Error |
|---|---|---|---|---|---|---|---|
| 1 | 298.15 | 1.02 | 1.03 | 0.32% | 53.40 | 54.45 | 1.96% |
| 2 | 298.15 | 0.90 | 0.70 | 22.74% | 43.93 | 27.44 | 37.53% |
| 3 | 298.15 | 0.98 | 0.87 | 1.84% | 45.00 | 46.46 | 3.24% |
| 4 | 298.15 | 1.04 | 1.04 | 0.01% | 39.60 | 43.43 | 9.69% |
| 5 | 298.15 | 0.86 | 0.86 | 0.71% | 42.25 | 41.39 | 2.02% |
| 6 | 318.15 | 1.05 | 1.08 | 2.43% | 56.32 | 59.83 | 6.24% |
| 7 | 298.15 | 0.79 | 0.81 | 2.69% | 29.63 | 31.25 | 5.47% |
| 8 | 298.15 | 0.84 | 0.61 | 27.88% | 30.9** | 31.33 | 1.05% |

References - Experimental data extracted from.[36–39]

Experimental value for 314 K

Therefore, the calibrated charge groups were used to built the scaffold of chalcones and flavonoids, or compounds **1** and **2**, respectively (Figure 1). The basic $C - H$ groups within benzene rings were set as $-0.13/+0.13$, respectivelly,[25] if not part of other substituent charge groups. Previously calibrated partial atomic charges from phenol and methoxybenzene were used for common substituents in natural products. In the case of vicinal substituents and overlapping atoms, the partial charge of such atoms were set as flexible in order to allow the MM dipole moment to be adjusted to the QM reference, but maintaining the core of the charge group.

As a next step, we evaluated how the torsional profiles obtained by QM for the selected building blocks were reproduced by the closest terms presented on GROMOS53a6 force field (Figure 2). For fragments **1**, **2**, **4** and **5**, torsional parameters tested were extracted from phenylalanine, parameters for phenol dihedral were tested for fragments **3** and **6**, while parameters of aspartate was tested for fragments **7** and **8**. It is clear from these results that non-specific torsional parameters may not always reproduce the quantum mechanics energy

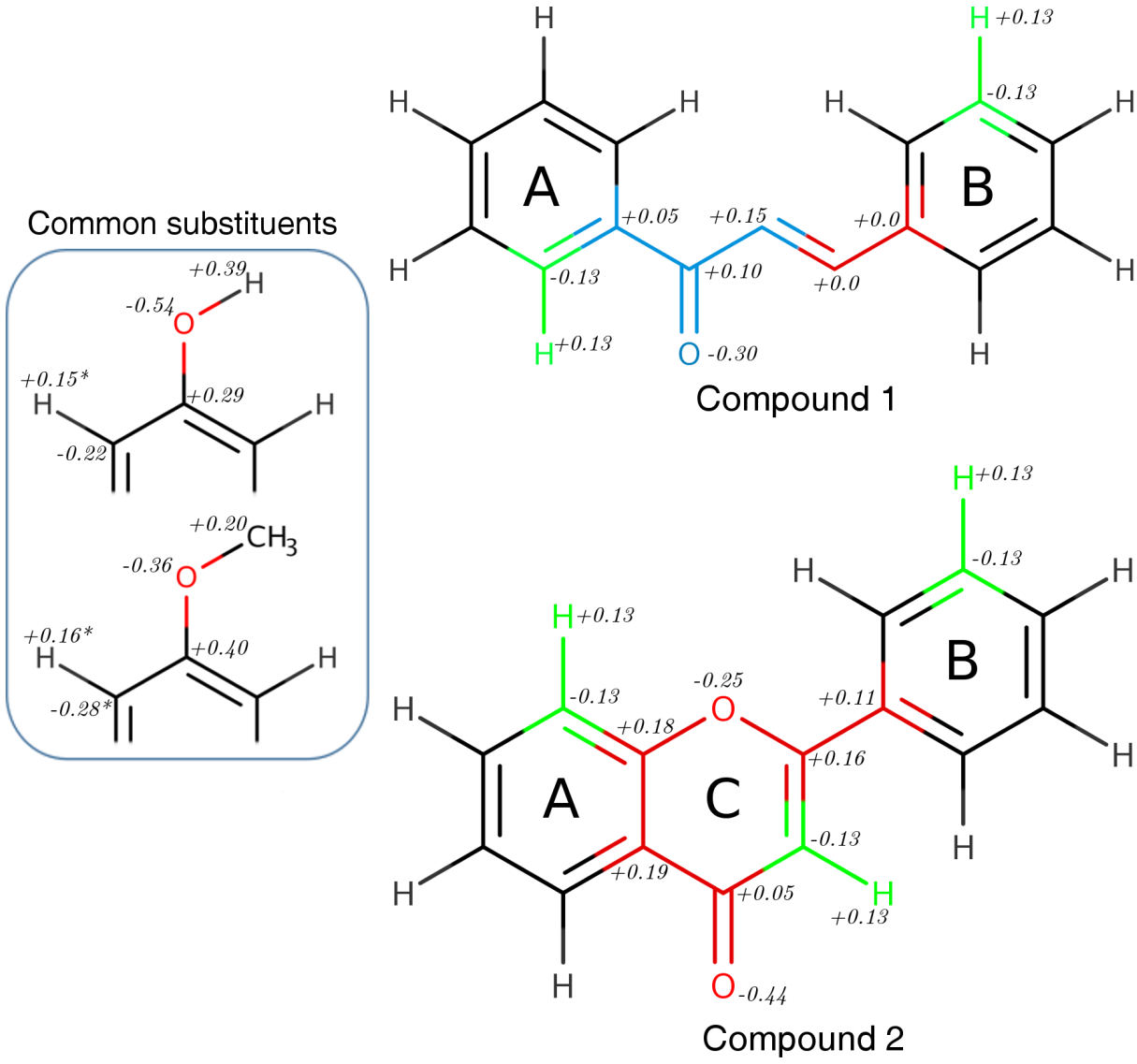


Figure 1: Colored charge groups used in this work for basic chalcones and flavonoids. Common substituents are also shown. Atomic partial charges marked with * stand for charges that are allowed to be modified in when superimposing vicinal substituents.

barriers and *minima* of a given dihedral, as expected. Although the automated approach is broadly used to treat ligands within ligand-receptor complexes,[40–43] uncured torsional parameters may strongly impact the accurate description of the conformational ensemble in free ligand molecular dynamics simulations, within the protein or even on receptors' conformational activation. To address this issue, new dihedral parameters potentials were generated (Table S1) and tested. The curves obtained using the new torsional parameters show good agreement with the respective values obtained by the QM calculations (Figure 2).

## Dynamics of Chalcones and Flavonoids

The topologies of the scaffold of chalcones and flavonoids previously built and calibrated were used, together with phenol and methoxybenzene atomic partial charges and torsional parameters, in order to build MD topologies for compounds **3, 4, 5, 6** and **7** (Figure 3). Considering these compounds have been previously characterized by NMR spectroscopy,[44–47] the inter-proton contacts (NOESY signals) were used to validate the conformational ensemble obtained from microsecond MD simulations. These simulations were carried out in organic solvent ($CHCL_3$ or DMSO) in order to reproduce the conditions of experimental procedures. Whenever a distance value was below a 5 Å cutoff, it was considered as a correct reproduction. In general, most of the experimentally observed contacts between the analyzed protons were properly reproduced in the simulations using organic solvents (Table 2) and water (Table S2), pointing to a precise conformational characterization of these compounds.

In order to investigate the conformational prevalences of chalcones and flavonoids dihedrals, we evaluated the distribution of the torsional angles adopted by the molecules during MD simulations (Figures 4 and 5). It is important to mention that all dihedrals analyzed here presented a high number of transitions between different angle populations, which suggests that our microsecond simulations were sufficiently long to sample most of the conformational states adopted by these molecules, and that it was not trapped in a single energetic *minimum*

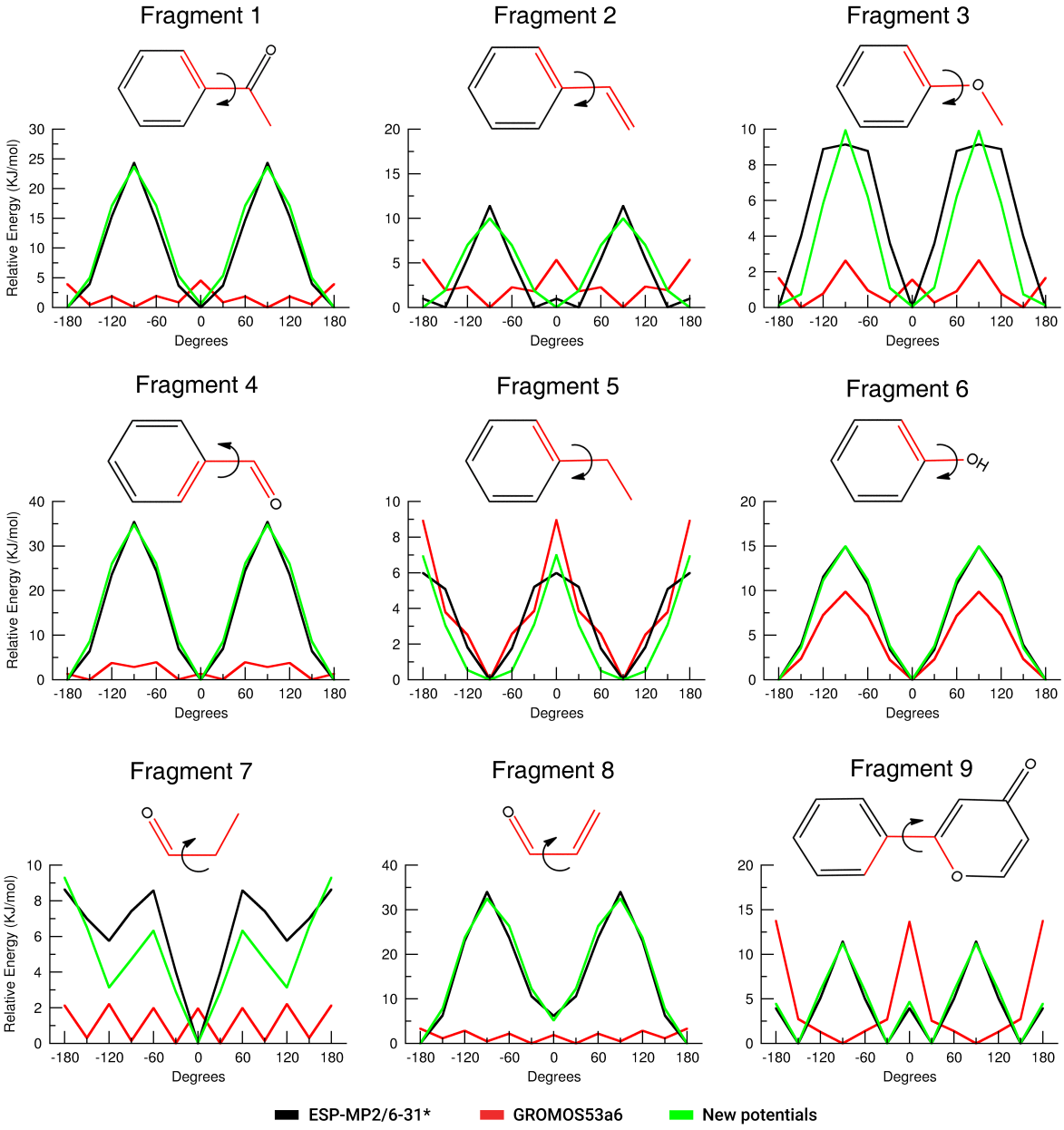


Figure 2: Comparison of MP2 6-31G* calculations (black) and MM torsional profiles of the structures with the adjusted terms accounting for 1-4 interactions (green) and with parameters for the most similar chemical pattern found in GROMOS53a6 (red).

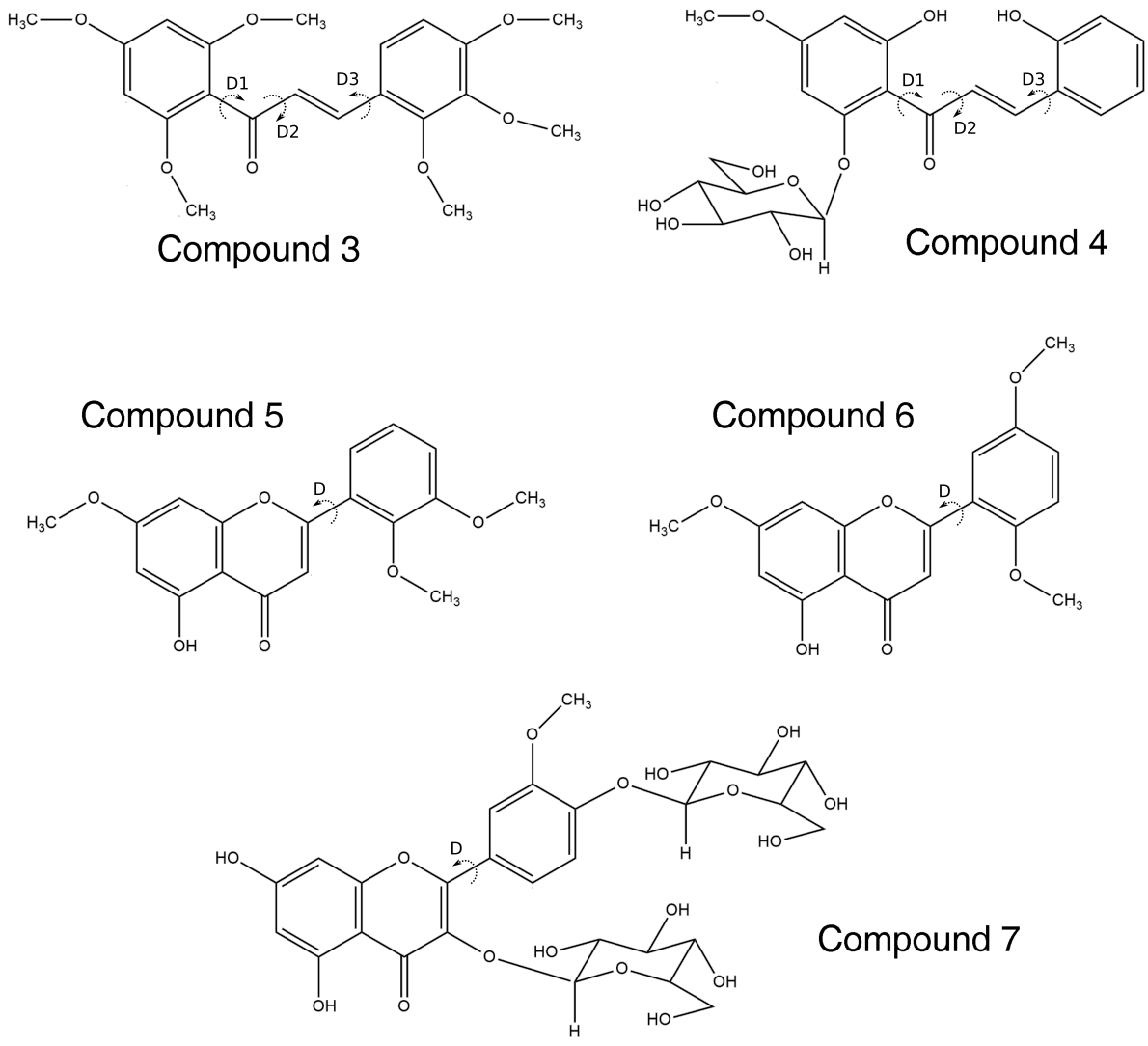


Figure 3: Chalcones and flavonoids employed in this work to validated the conformational ensemble obtained by MD simulations, using experimental NOESY signals.[44–47]

(Figures S2-S4).

The chalcone structure has proven to be very flexible around the dihedrals between rings A and B, as the geometry distribution demonstrated the population of at least 2 preferential states for each torsion (Figure 4). The chalcone without substituent groups in the aromatic rings (compound **1**) presented a single most abundant conformational state for all dihedrals, as a consequence of the ring symmetry. On the other hand, methoxy groups in *ortho* (compound **3**) caused a deviation of ± 90° in D1, 180° in D2 and shift the the most abundant D3 angle to 180°. In the case of compound **4**, the monosaccharide residue broke the ring symmetry and completely changed the most abundant conformational states for D1, shifting it to a −150° angle and a minor population on 150°. For D2, a second population in 180° had an increased frequency when simulating compound **4** in water, in comparison to the non-substituted chalcone (compound **1**), which can be explained by a transient H-bond bridged by water between the monosaccharide and the hydroxyl group in ring B, and explains the lower frequency observed for D2 of compound **4** simulated in DMSO solvent. For D3, a single hydroxyl group in *ortho* of B ring was sufficient to substantially reduce the 180° populations observed for compound **1**.

The flavonoid scaffold has only one torsion and can be considered more rigid then the chalcones studied here. Still, differences can be noticed regarding different vicinal substituent patterns (Figure 5). The dihedral D of the non-substituted flavonoid (compound **2**) has a rapid interconversion from −15° to 15° angles, which could be misread as a continuous population of 0°. In fact, our QM calculations of fragment **9** has shown energy *minima* around such values, in addition to ± 150°, also in agreement with previous works.[48–50] The addition of a vicinal methoxy group (compounds **5** and **6**) extinguished the population on ±15° and shifted the major populations to ±150°. The addition of a sugar moiety also in to the dihedral (compound **7**) eliminated the population with D=150° due to sterical clashes between methoxy group and the monosaccharide, preserving only the population at D=−150°.

The distribution of glycosidic linkages during the MD, on compounds **4** and **7**, exhibited single distribution on $\phi$ and $\psi$ angles (Figures S7 and S8), demonstrating a rigidity for these glycosidic linkages. On compound **4**, both dihedral angles revealed only one conformational state ($\phi$=$-60°$ and $\psi$=$-60°$) (Figure S6). On compound **7**, both $\phi_1$ and $\phi_2$ dihedrals revealed a single distribution at $-60°$ and $-90°$, respectively, while $\psi_1$ showed a bimodal distribution ($\pm 90°$) and $\psi_2$ revealed a single distribution also around $-90°$. It is important to notice that the $\psi_1$=$90°$ is related to a H-bond between the hydroxyl groups of monosaccharides units, which explains the higher frequency of this angle during MD simulations.

For all compounds, the reproduction of dihedral distributions had little difference during simulations in both aqueous and organic solvents. In specific cases, as in D1 and D2 of compound **4**, water molecules mediated intramolecular interactions that increased minor populations observed in simulations in DMSO solvent.

**Table 2: NOESY contacts of compounds, inter-proton distances derived from microsecond MD simulations in organic solvents**

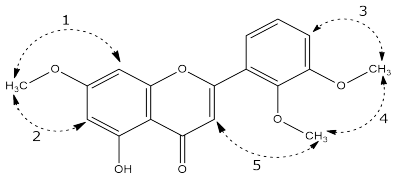

Compound 5

| NOE | Av. Distance (Å) |
|---|---|
| 1 | 4.06 ± 0.39 |
| 2 | 2.54 ± 0.76 |
| 3 | 3.11 ± 0.66 |
| 4* | 4.55 ± 0.67 |
| 5* | 4.07 ± 0.40 |

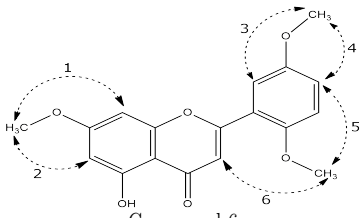

Compound 6

| NOE | Av. Distance (Å) |
|---|---|
| 1 | 2.78 ± 0.73 |
| 2 | 3.60 ± 0.50 |
| 3 | 3.36 ± 0.54 |
| 4 | 3.10 ± 0.67 |
| 5* | 5.11 ± 0.74 |
| 6* | 3.71 ± 0.38 |

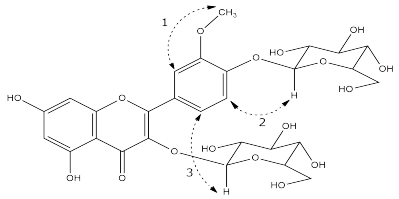

Compound 7

| NOE | Av. distance (Å) |
|---|---|
| 1 | 2.21 ± 0.86 |
| 2* | 2.73 ± 0.26 |
| 3* | 4.35 ± 0.52 |

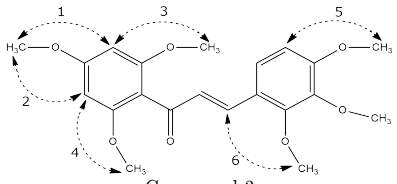

Compound 3

| NOE | Av. Distance (Å) |
|---|---|
| 1 | 3.58 ± 0.60 |
| 2 | 2.97 ± 0.72 |
| 3 | 2.94 ± 0.70 |
| 4 | 2.24 ± 0.79 |
| 5 | 2.18 ± 0.86 |
| 6* | 3.04 ± 0.67 |

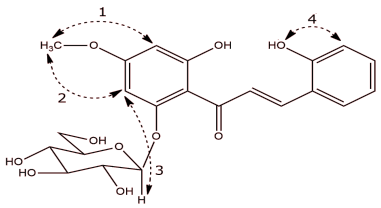

Compound 4

| NOE | Av. Distance (Å) |
|---|---|
| 1 | 2.55 ± 0.80 |
| 2 | 4.04 ± 0.24 |
| 3* | 2.30 ± 0.25 |
| 4 | 2.23 ± 0.25 |

*NOESY contacts that could be above 5 Åduring the MD simulations.

The average distances were computed as $\langle r^{-6} \rangle^{-1/6}$, respecting the NOE intensity for small molecules.

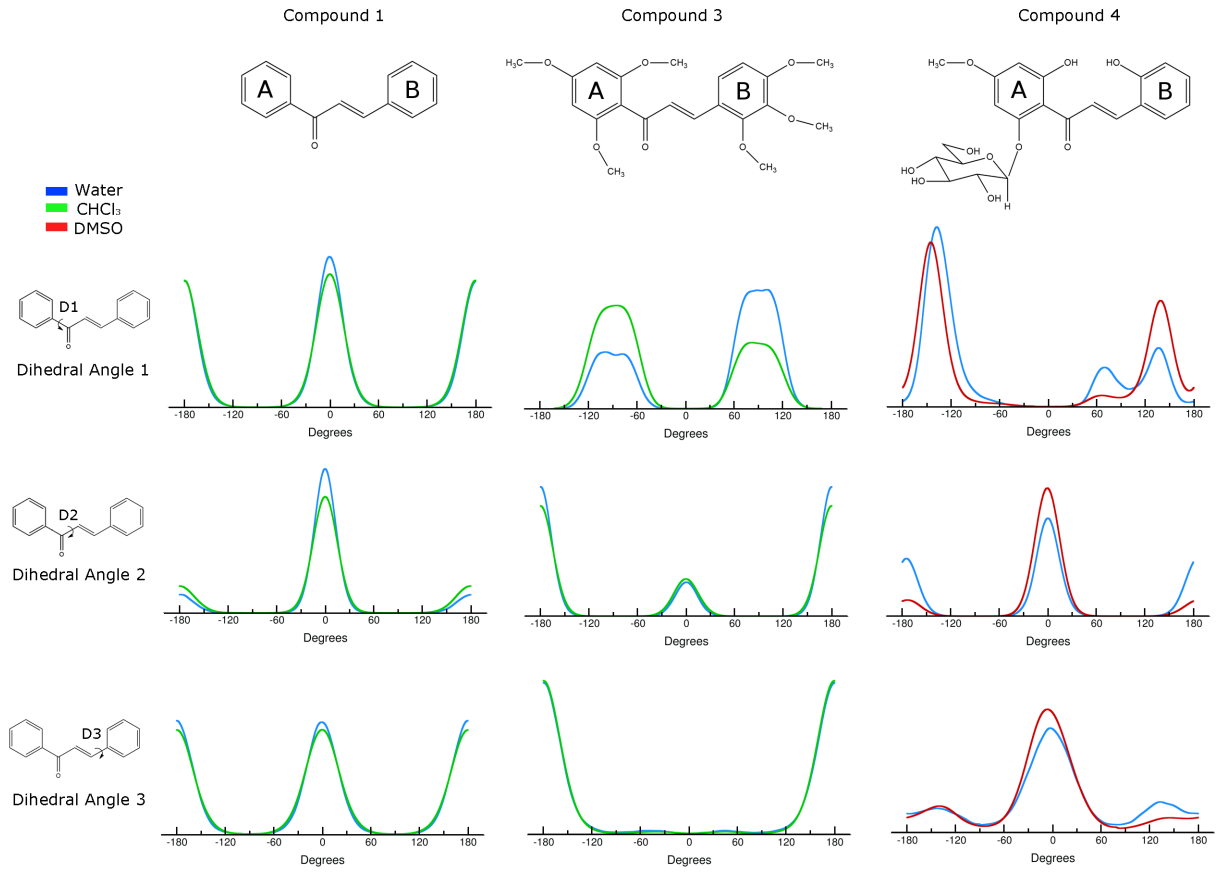


Figure 4: Distribution of the dihedral angles within the main chalcone structure during microsecond MD simulations.

## Energetic effects of substitutions and solvent

In order to evaluate the effect of different substituents and solvents in the torsional barriers specifically designed in this work for flavonoids and chalcones, a series of metadynamics calculations[51–53] were performed for each dihedral angle separately or in vicinal couples, both in water and in organic solvent ($CHCL_3$ or DMSO).

On chalcones fragments (**10-12**), dihedrals D1 and D2 were used as collective variables (CV) to calculate the free-energy surfaces of their torsions. Our results show that additions of different groups on the external rings can modify the torsional free-energy associated to the dihedrals adjacent to the carbonyl group (Figure 6 and 7). When compared to fragment **10**, the torsional profile of D1 in fragments **11** and **12** suffered major modification, both in the

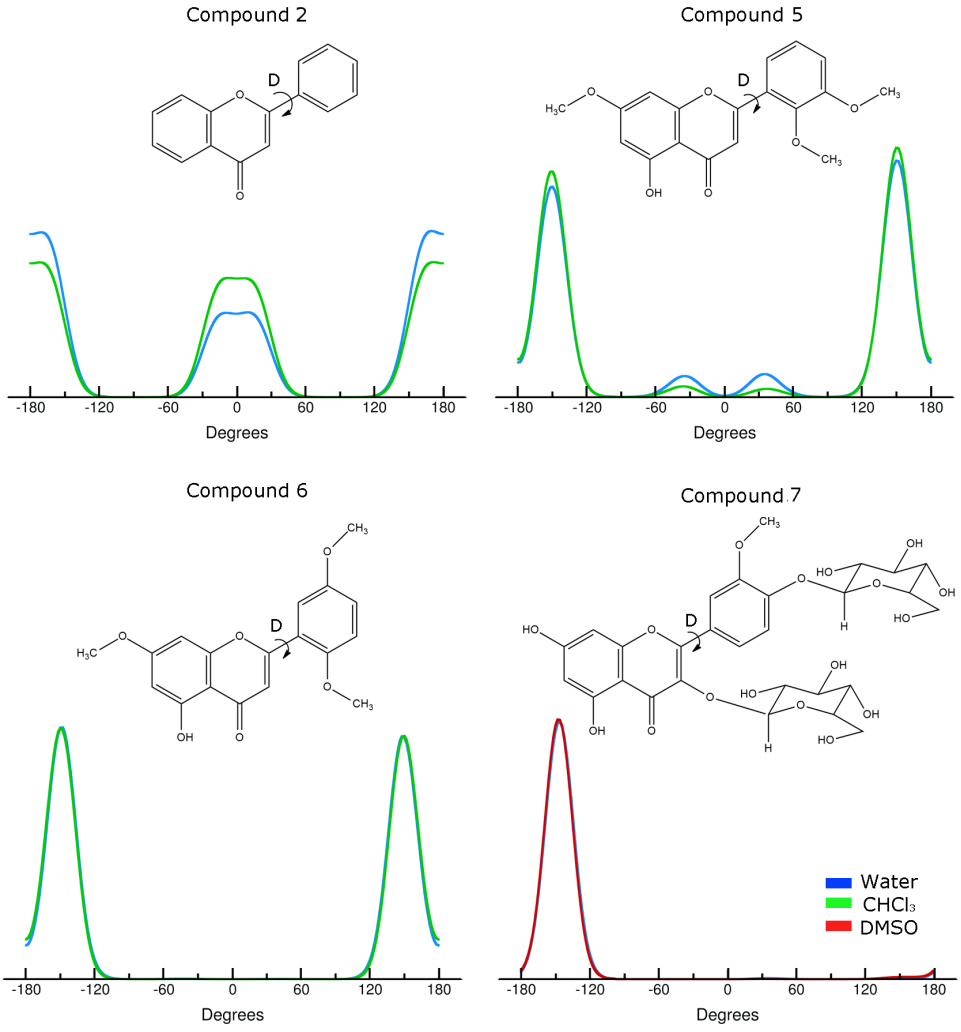


Figure 5: Distribution of the main dihedral angle associated with the linkage between the rings on flavonoids structures during microsecond MD simulations.

energetic barrier and number of *minima*. For fragment **11**, the presence of methoxy groups vicinal to the dihedral shifted the energetical minimum from D1 to ± 90° and increased the torsional activation energy from 20 kJ/mol to 60 kJ/mol, most likely due to the steric hindrance of such substituents. For D2 in fragment **11**, the addition of methoxy groups decrease the torsional activation energy in 10 kJ, shifting the dihedral frequency to 180°, as seen in Figure 4.

For fragment **12** in DMSO, the presence of the monossacharide near dihedral D1 induced a shift of the free-energy minimum to −135° and a local minimum of 135°. In the case of dihedral D2, the monossacharide increases the free-energy of −180°, increasing the dihedral population at 0°. However, simulations in water revealed a new energetical minimum in D1=75° due to the increase on the free-energy at 135°, which substantially reduces the energetical barrier between the two populations, yielding an increase in the frequency of D1=75° for compound **4**, as shown in Figure 4. In addition, the dihedral distribution of the complete molecules in water revealed an increased population of D2 in ±180°. The new torsional angle of D1=75° allows a H-bond mediated by water between the sugar moiety and the hydroxyl group in ring B, increasing frequency of D2=±180°. These results suggest that the organization and strength of solvent interactions around flexible molecules can substantially influence their uncomplexed dynamics in solution.

The energetic impact of different ring substitutions and solvents were evaluated for dihedral D3 in compounds **1**, **3** and **4** using dihedral D3 as CV. Metadynamics calculations of compound **1** in water and $CHCL_3$ are in accordance with the QM and MM torsional profile generated for fragment **2**, with free-energy *minima* in 0° and 180°. However, the presence of a vicinal methoxy group (compound **3**) extinguished the minimum in 0°, inducing the preferential conformation at D3=±180° both in water and $CHCL_3$. In the case of compound **4** in DMSO, the presence of a vicinal hydroxyl group maintain the 0° minimum while increasing the free-energy at 180°, also increasing the preference for torsion D3 at 0°. Despite that, simulations in water showed a new local *minimum* at ± 140°, with a decrease

around 10 kJ/mol in comparison to DMSO simulations. Further investigations revealed an intermolecular interaction between the sugar moiety and hydroxyl group in ring B mediated by 1 or 2 water molecules, which explains the slight increase of D3 population at 140°. Still, the preferential conformation of D3 remained fixed around 0° and a large deviation of ±40°.

Aiming to evaluate the energetic impact from torsions of nearby substituents on flavonoids, metadynamics calculations were also performed for compounds **2**, **5**, **6** and **7** (Figure 8) using the dihedral D as CV. Calculations of compound **2** showed angular *minima* at ±30° and ±150°, in accordance to the torsional profile calculated *in vacuo* by QM methods for fragment **9**. It is important to notice the low energetic barrier between 30° and −30° or 180° and −180°, which explains the rapid interconversion between these close *minima*. However, the addition of a methoxy group near the dihedral D (compound **5**) extinguished the minimum at ±30° and shifted the global minimum from ±180° to ±145°. Still, a minor population at D=±30° can be observed in Figure 5, which can be explained by the low barrier between the global and these local *minima* at 30°. For compound **6**, the presence of a second methoxy group in *para* did not change the global or local energy *minima*, but increased the free-energy barrier from 6 kJ/mol to 22 kJ/mol while increasing the content of free-energy when D=45°. For compound **7**, the presence of a sugar moiety in *ortho* to the dihedral maintained the global minimum at −150° while creating a new local minimum at D=30° due to the torsional asymmetry. Even though transitions could be observed between these *minima*, the dihedral distribution of D in compound **7** showed a complete preference for −145°±20° due to intramolecular H-bond between the sugar moieties.

Also, the free energy profiles associated to the $\phi$ and $\psi$ dihedrals of sugar moieties in compounds **12**, **13**, **14**, **15** (Figures S5 and S6) suffered minor influences from the different solvents, yielding similar *minima* regions on their free-energy torsional landscapes. In a particular note, $\psi_1$ on compound **7** revealed a bimodal distribution on angles 90° and −90°, in contrast with $\psi_2$. This can be explained by a intramolecular H-bond between the sugar moieties when $\phi_1$=90° which maintained $\phi_2$ at −90°.

The data gathered here regarding the effect of nearby substitutions and the possible solvent effects in torsional free-energy barriers can be of interest for medicinal chemists while designing new ligands or increasing the potency of old ones. In fact, mapping such torsional free-energy profiles can also be useful to predict likely and unlikely conformations of ligands *a priori*, a challenging task when starting from 2D chemical structures.

## Dynamics in Solution

The broad biological activities of natural products in traditional folk medicine[4–12] has increased the interest of medicinal chemists to comprehend the basis of molecular recognition at the ligand-receptor complex level. Thus, the knowledge of conformational preferences of bioactive compounds in solution is not only relevant to predict the enthalpic and entropic costs of binding, but also to evaluate possible conformational selection or induced fit mechanisms of recognition, which in turn provide valuable insights for rational drug design.

In this sense, we have generated torsional parameters for chalcones and flavonoids that yielded good agreement with QM calculated torsional profiles. Moreover, atomic partial charges were calibrated for chalcone and flavonoid scaffolds, as well as for common substituents, using experimental thermodynamic properties from organic liquids as targets. Topologies built with such parameters yielded good agreement with inter-proton NMR data during molecular dynamic simulations, which reinforces the accuracy and reliability of our parameters to allow conformational and energetical studies of chalcones and flavonoids.

With these results in hand, the conformational sampling of compounds **1-7** was evaluated during microsecond classic molecular dynamics simulations, which allowed the identificaton of their main conformational states in water and organic solution, which were compiled in Tables S3 and S4.

For compound **1**, there are two main conformational statesin both solvents (Figures 9A and 9B). The most abundant conformation for this chalcone in $CHCL_3$ is related to a energetical preference of D2=0°, as discussed above, yielding an abundance of nearly

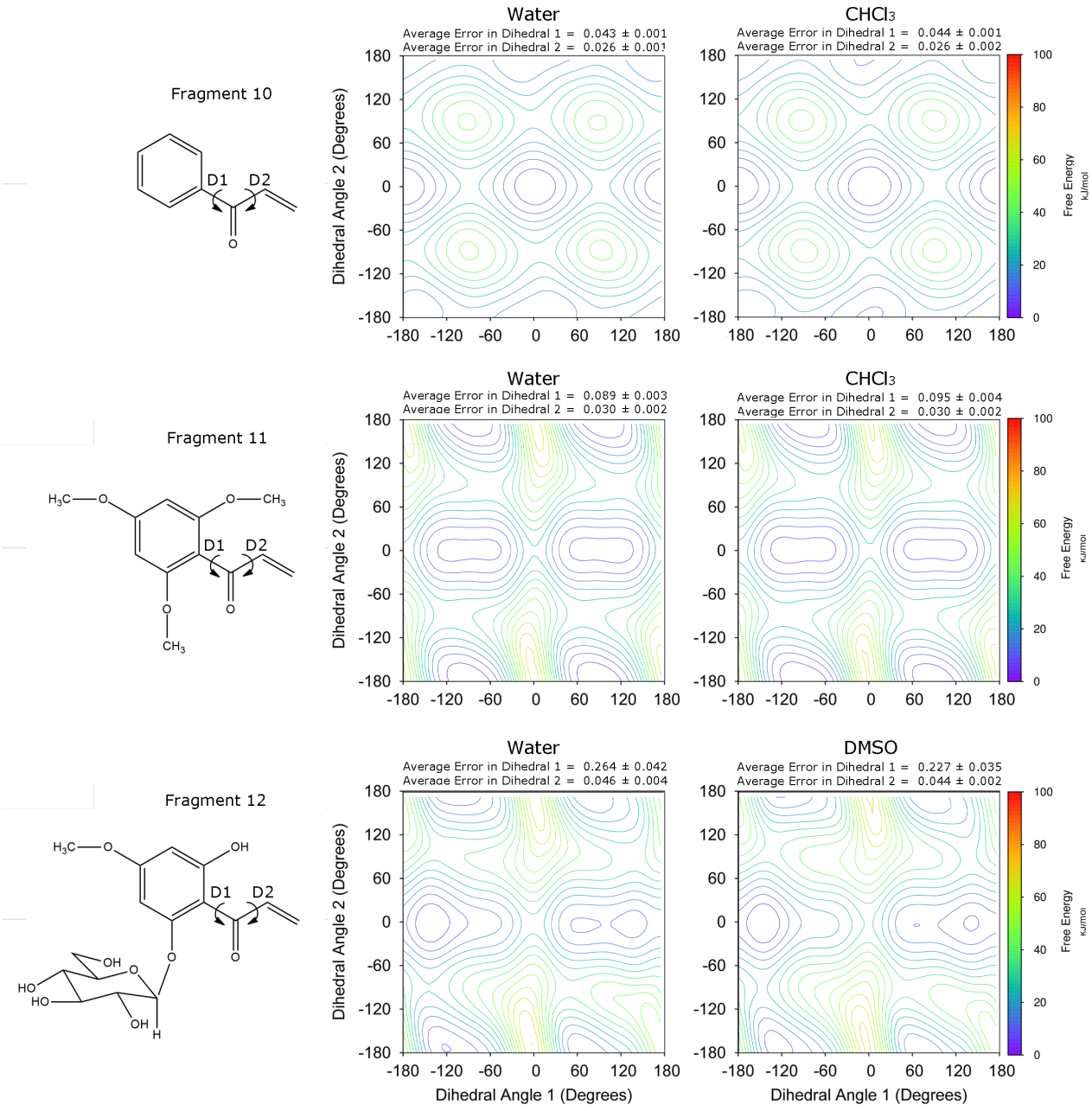


Figure 6: Free energy profiles obtained from metadynamics simulations for the dihedral angles 1 and 2 on fragments **10**, **11** and **12**, related to the main structure of the chalcone scaffold.

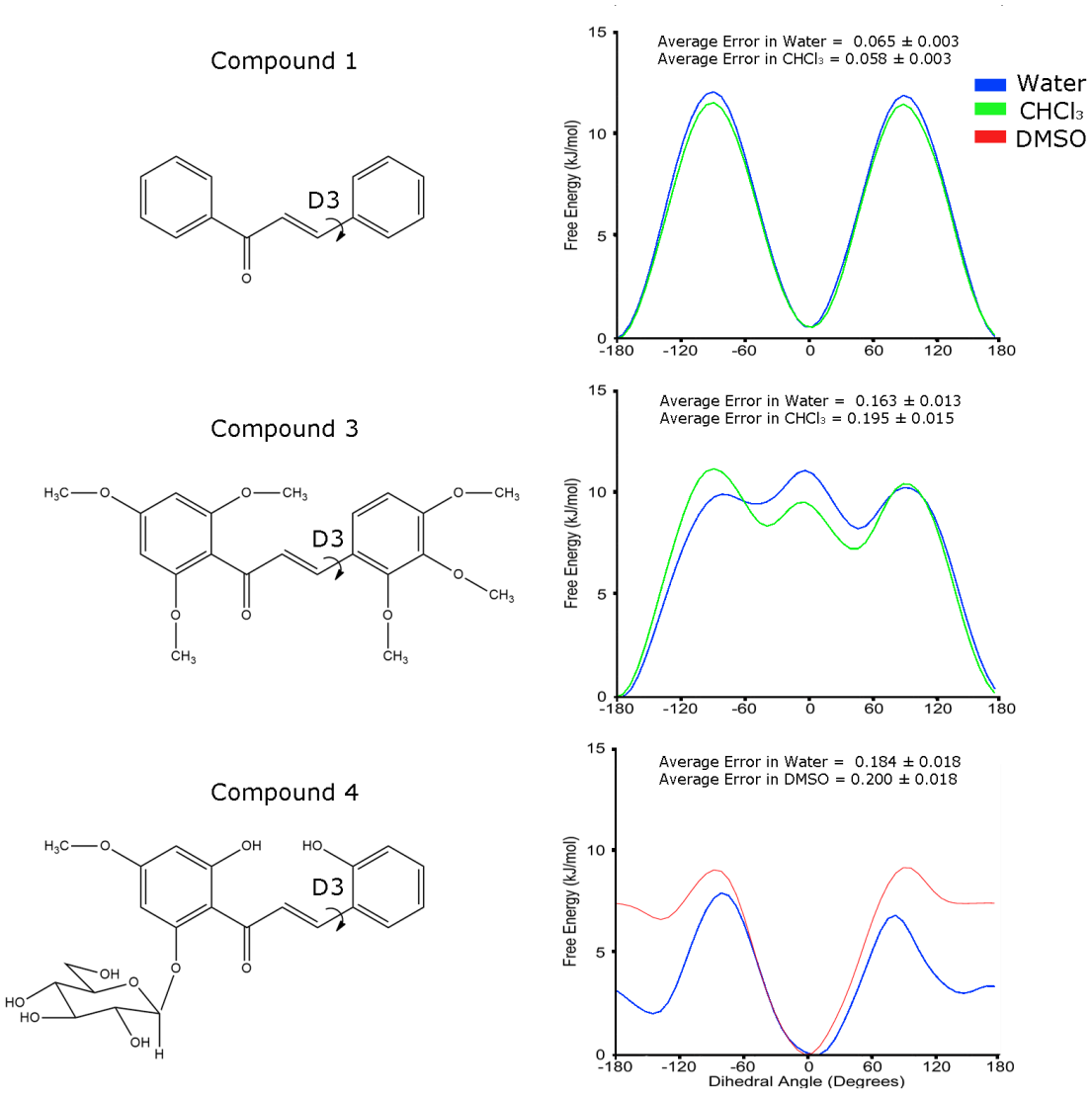


Figure 7: Free energy profiles obtained from metadynamics simulations for the dihedral angle 3 on compounds **1**, **3** and **4**.

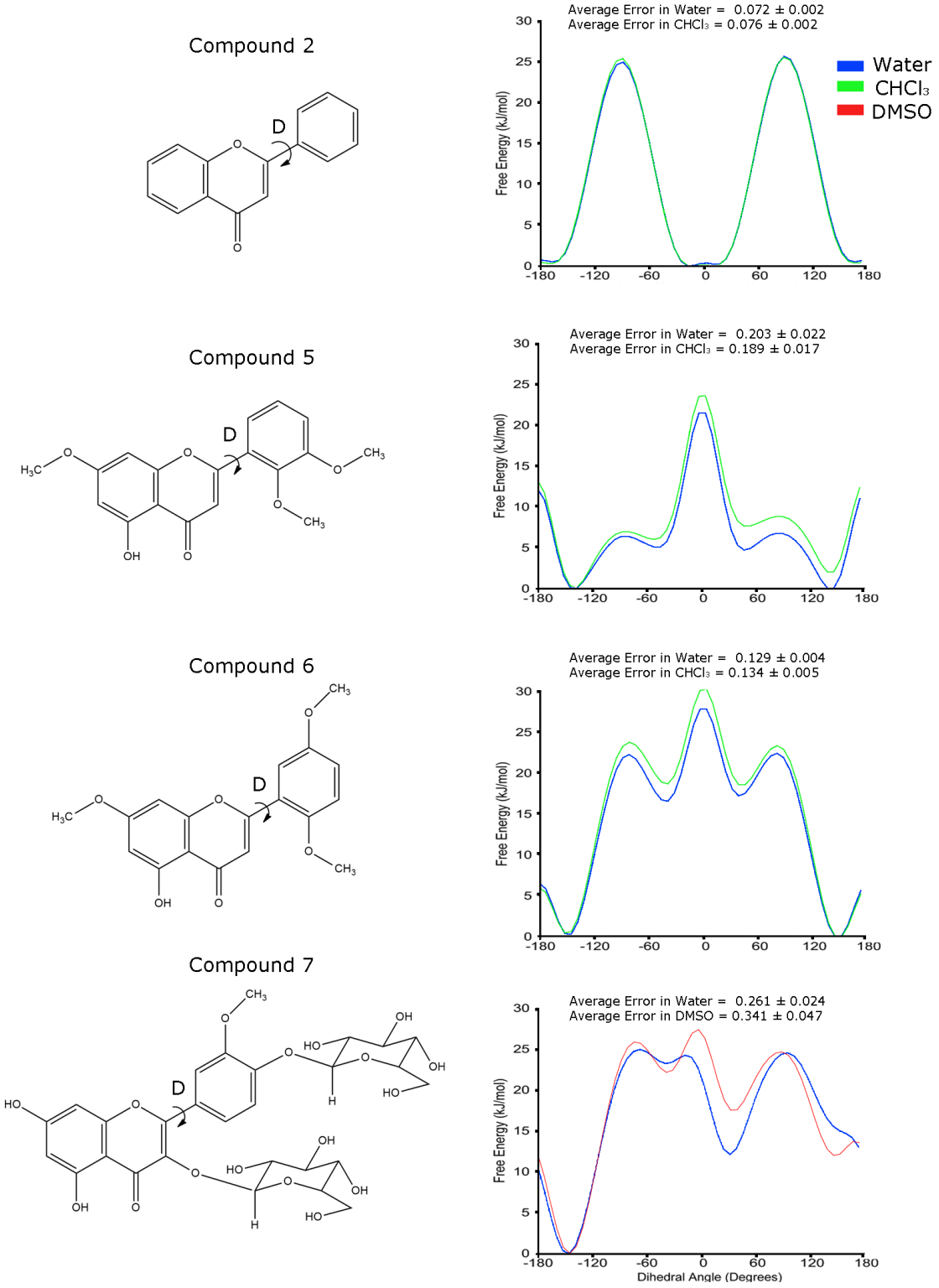


Figure 8: Free energy profiles obtained from metadynamics simulations for the main dihedral angle of compounds **2**, **5**, **6** and **7**.

80%, while D2=±180° accounts for 20%. In water, these abundances are 85% and 15%, respectively. For compound **3**, the opposite behavior is presented on both solvents when compared to molecule **1**. Aside from the ±90° angle for D1, dihedral D2 in compound **3** presented a preference for ±180°, with an abundance of nearly 80% in both organic and water solution. On compound **4**, there are different behaviors for each solvent. In DMSO, three conformational states were found, while four conformations were identified in water (Figures 9A and 9B), although the main conformations found in both solvents were equivalent (with abundances of 35% and 23%, respectively). Moreover, the second population in DMSO (D1=140°,D1=0°,D1=0°) with an abundance of 32% represents only 9% of the populations in water, the third most abundant conformation. The second most abundant population in water is stabilized by a water mediated H-bond between the sugar moiety and the hydroxyl in chalcone ring B (data not shown), thus explaining the 15% abundance. The glycosidic linkage showed the same value for all conformations (Table S3), according to previous analyzes of $\phi$ and $\psi$ angles, demonstrating only one abundant conformational state (Figura S6). It is important to notice that, while the conformational profile of compound **4** described here accounts for nearly 80% of the total conformations obtained by MD simulations in DMSO, we were able to identify only 47% of the conformations obtained in water solvent (Table S3). These results suggest that the addition of sugar moieties increase the flexibility of chalcones, specially when capable of intramolecular interactions, by stratifying the major identifiable conformations.

In general, flavonoids presented the same conformational populations on both solvents (Figures 10A and 10B), and the combination of the most common conformational populations were compiled in Table S4. Compound **2** presented only one conformational state in solution with dihedral D=±30°, with rapid interconversion and low free-energy barrier between these conformational states. On the other hand, the most common conformational populations for compounds **5** and **6** could be identified at D=±150°, with nearly 50% for each dihedral angle. As previously seen, the methoxy group on the rings of molecules **5** and **6** influenced on these

conformational profiles, explaining these news configurations when compared to compound **2**. Despite the main dihedral angle on compound **7** showing the same conformational states for all conformations (Table S4), the analyses of the relative abundances of each dihedral indicated two conformations for $\psi_1$ angle, between $\pm 90°$ (Table S4). The preference for $\psi_1 = 90°$ is related to a transient intramolecular H-bond between the sugar moieties (data not shown). This data is in accordance with previous analysis (Figure S8) that showed two conformational states for this dihedral angle.

The conformational sampling obtained here was also capable to describe the conversion between different conformational states. So, in the context of conformational selection recognition mechanism for small ligands, such strategy may represent an useful methodology to contribute in the choice of ligands conformations for future studies, such as 3D-QSAR and docking calculations. In the context of induced fit recognition mechanism, the previous knowledge of free-energy torsional surfaces can provide quantitative data to the energetic cost of fitting a given pharmacophoric region by twisting scaffold main dihedrals.

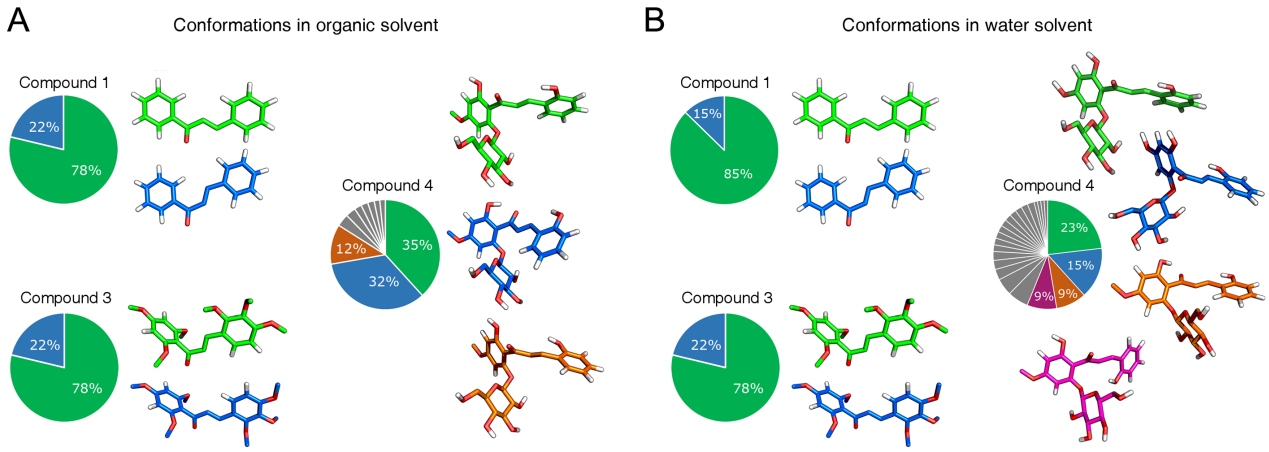


Figure 9: Abundance of different conformations of chalcones during microsecond MD simulations performed in organic solvents (A) and water (B) for compounds **1**, **3** and **4**.

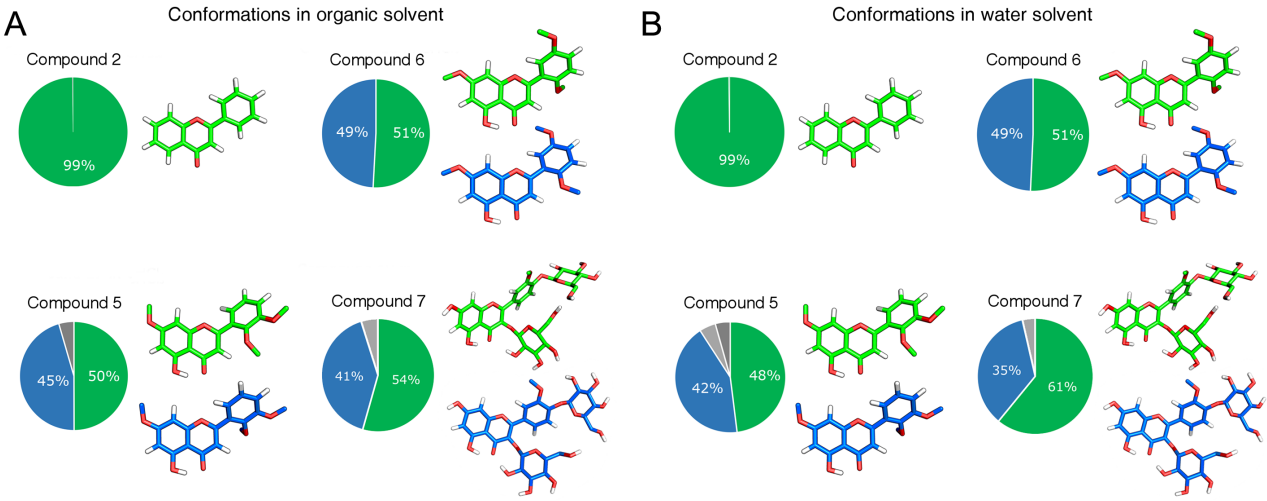


Figure 10: Abundance of different conformations of flavonoids during microsecond MD simulations performed in organic solvents (A) and water (B) for compounds **2**, **5**, **6** and **7**.

# Conclusions

In the current study, a new parameter set for force field calculations of chalcones and flavonoids was presented, in which we included new torsional potentials within GROMOS force field, as well as a set of atomic partial charges. The major advantage over previously proposed modifications of the force field is that this approach is still compatible with the general GROMOS parameter set for other classes of biomolecules, allowing prompt simulations of ligand-receptor complexes. The addition of new torsional potentials is a similar approach to that performed for improving GROMOS parameters for proteins,[54,55] carbohydrates[56] and aromatic rings commonly used in drug design,[25] which allows a state-of-art description of conformational profile of ligands. The generated parameters for the description of small molecules reproduce well QM and experimental data, while microsecond MD simulation of complete chalcones and flavonoids were capable of reproducting experimental interproton NOE contacts, suggesting a precise conformational characterization for these molecules. This allowed us to evaluate the energetic impact of common ring substitutions on the free-energy torsional profile of each main dihedral on chalcones and flavonoidic scaffold, as well as the effect of solvent substitution on such energies. Moreover, we were able to

identify the most common conformational populations of these molecules in both organic solvent and water, providing quantitative information for medicinal chemists in rational drug design efforts. This set of parameters and the conformational sampling of chalcones and flavonoids are expected to contribute in future studies, supplying accurate results through MD simulations.

# Experimental

## Derivation of new torsional parameters

The QM torsional profiles of dihedrals within the structures were obtained using Gaussian03.[57] These QM calculations were carried out using the *scan* routine combined with a *tight* convergence criterion, at MP2 level with the 6-31G* basis set, obtaining the relative energy associated with the rotation of each dihedral by increments of 30°.

The potential energy term associated with the torsion around a dihedral angle $m$ in MM calculations is described by the following equation, where $\phi_{\mathrm{m}}$ is the dihedral angle value, $n_{\mathrm{m}}$ is the multiplicity of the term, $\delta_{\mathrm{m}}$ the associated phase shift, and $k_{\phi,\mathrm{m}}$ the corresponding force constant:

$$V_{\phi,m} = k_{\phi,m}[1 + cos\delta_m cos(n_m\phi_m)] \quad (1)$$

Hence, MM calculations were performed in GROMACS 5.0.7 for every dihedral angle evaluated by previous QM methods, evaluating the total potential energy related to the conformation, including 1,4 nonbonded interactions.[56,58] Both QM and MM torsional energies were then submitted to the Rotational Profiler server,[59] which calculates the energy gap between both profiles and provides proper MM torsional parameters fitted to the QM. These new parameters were then properly implemented into the topologies for MD simulations.

## Parametrization strategy and topology construction

In order to describe chalcones and flavonoids through molecular mechanics techniques, a set of aromatic rings with substituents commonly found in chalcones and flavonoids was selected as building blocks. The parametrization strategy was based on accurately reproduce experimental values for physicochemical properties of organic liquids. Topologies were constructed for the fragments using the potentials for bond stretching, bond-angle bending, and improper dihedral deformation, as well as van der Waals interactions terms retrieved directly from GROMOS53A6[27] set. In order to obtain atomic partial charges, QM calculations were performed using Gaussian09,[57] at the second-order Møller-Plesset perturbation (MP2)[60] level with the 6-31G* basis set, in implicit PCM (polarizable continuum model) solvent,[61] followed by a RESP fitting.[62] Charge adjustments were made to properly reproduce the experimental properties in MM conditions, taking care to maintain the dipole moment direction obtained from QM calculations, using a in-house tool based on Least-squares fit solution (available in Supplementary Material). All of the MD simulations and analyses were performed using the GROMACS simulation suite,[63] version 5.0.7.[64]

In order to derive the charge for the entire chalcone or flavonoid molecule, larger fragments were used. Atomic group charges of the common substituents previously calculated were used and, in case of overlapping group charges, adjustments were carried in order to maintain the total dipole moment of the fragment. Therefore, entire molecules were built by adding these fragments as building blocks *per se*, allowing us to describe differently substituted chalcones and flavonoids.

## Least-squares fit solution

The adjustment of charges while keeping the total dipole moment of a molecule was modeled as a linear least-squares problem with bounds on the variables[65,66] and solved using the SciPy[67] library from the Python 2.7 programming language.

In this scheme, $x$, $y$ and $z$ atomic coordinates are obtained from a SYBYL MOL2 format

file generated after a MP2/6-31G* calculation, along with their respective partial charges derived from a RESP fitting. Thus, in this modeling, all $n$ atoms form a matrix $A$ of atomic positions, with $a_n^x$ being the $x$ coordinate of atom $a_n$ and so on.

$$A = \begin{bmatrix} a_1^x & a_2^x & \dots & a_n^x \\ a_1^y & a_2^y & \dots & a_n^y \\ a_1^z & a_2^z & \dots & a_n^z \end{bmatrix}$$

$C_{ref}$ is the vector of partial charges obtained from QM calculations, and $r_n$ is the reference charge of atom $a_n$.

$$C_{ref} = \begin{bmatrix} r_1 & r_2 & \dots & r_n \end{bmatrix}^T$$

$K$ is the dipole moment from QM calculations charges and $\cdot$ is the dot product.

$$A \cdot C_{ref} = K$$

$L$ is the vector of lower bound values for the new charges, with $l_n$ being the lower bound of the new charge of atom $a_n$, while $U$ is the vector of upper bound values for the new charges and $u_n$ is the upper bound of the new charge of atom $a_n$.

$$L = \begin{bmatrix} l_1 & l_2 & \dots & l_n \end{bmatrix}^T$$

$$U = \begin{bmatrix} u_1 & u_2 & \dots & u_n \end{bmatrix}^T$$

$Q$ is the coefficient vector used to change the magnitude of the dipole moment $K$.

$$Q = \begin{bmatrix} q_1 & q_2 & \dots & q_n \end{bmatrix}^T$$

From this, it is intended to find the vector of new charges $C$, such as $c_n$ is the new charge of atom $a_n$, using the linear least-squares method.

$$C = \begin{bmatrix} c_1 & c_2 & \dots & c_n \end{bmatrix}^T$$

Vector $C$ is the solution of the system: $A \cdot C = K \circ Q$

With restraints: $\sum_{i=1}^{n} c_i = m$ and $\forall c \in C, l_c \leq c < u_c$

In which $\circ$ is the Hadamard product (element-wise multiplication), and $m$ is the total charge of the molecule. This assures that the new set of charges $C$ maintains the original dipole moment direction and total charge of the molecule from $C_{ref}$, while also respecting the lower and upper bounds and altering the magnitude of the new dipole moment. The main advantage of this approach is that it allows a combination of the transferability principle of calibrated atomic charge groups while respecting the dipole moment direction obtained from QM calculations.

## Liquid and gas-phase simulations for assessment of thermodynamic properties

Physicochemical properties of organic liquids (density and enthalpy of vaporization) were used as target to validate our topologies, as previous works of parametrization of small biomolecules[24,26,32] and benchmark of force fields.[25,35] The protocol described in Horta *et al.*[24] was applied to all building blocks containing functional groups necessary to the assembly of complex chalcones and flavonoids. These fragments were chosen considering the availability of experimental values of density and enthalpy of vaporization, and the topologies were accepted as useful when the absolute error between experimental and simulated properties properties was below 15%.

In order to calculate thermodynamic properties of organics liquids, a condensed phase was induced by simulating a 125 molecules under 100 bar. The box was scaled 2×2×2 in order to obtain 1000 molecules in liquid phase. All simulations were carried out with Berendsen pressure and temperature coupling algorithms[68], using $\tau_T = 0.2$ ps and $\tau_P = 0.5$ ps, along with reaction-field method to compute electrostatic interactions[69,70] using $\epsilon_{RF}$ as the experimental dielectric constant,[24,27] while the experimental isothermal compressibility was used as an additional parameter when available[24,27]. Otherwise, the compressibility of the most chemically similar molecule was used. While liquid-phase simulations were carried

out for 10 ns using *leap-frog* algorithm, gas-phase simulations were performed using stochastic dynamics algorithm[71] to simulate a single molecule in vacuum for 100 ns. *LINCS* algorithm was applied to constrain all bonds. The potential energies associated with these systems ($E_{pot}(g)$ for gas-phase and $E_{pot}(l)$ for liquid-phase) were extracted and used to calculate (Eq. 2) the enthalpy of vaporization ($\Delta H_{vap}$) of the fragments.

$$\Delta H_{vap} = (E_{pot}(g) + k_B T) - E_{pot}(l) \quad (2)$$

Organic liquid densities ($\rho$) were calculated from liquid-phase simulations using block averages of 5 blocks, as for $\Delta H_{vap}$. MD simulations were carried out by means of the GROMACS 5.0.7 package, and all the analyses employed dedicated tools from the GROMACS package, associated with in-house scripts to calculate thermodynamic properties.

## Metadynamics simulations

For the structural assessment of complete chalcones and flavonoids, metadynamics simulations were performed in order to determine the conformational preferences of dihedral angles in the main scaffold of these compounds and the associated carbohydrate moieties. Several fragments containing the dihedrals of interest were constructed and simulated during 50 ns, at 298 K and in nonaqueous solvents (chloroform or DMSO, to reproduce the conditions of the NMR experiments concerning the chosen complete chalcones and flavonoids) and water, as a control, in cubic boxes using periodic boundary conditions. The systems were submitted to energy minimization by steepest Descents algorithm, followed by an equilibration phase of 2 ns and subsequently to well-tempered (WT) metadynamics simulations. Gaussian hills with an initial height of 1.2 kcal.mol$^{-1}$ were applied, along with a hill width of 0.35 radians. In this WT scheme, Gaussian functions were rescaled employing a bias factor of 10. Pressure was kept constant at 1 atm by a Parrinello-Rahman barostat,[72,73] with a 2.0 ps coupling constant, and temperature was kept constant by a V-rescale thermostat (NVT step), with a

coupling constant of $\tau = 0.1$. The Lincs method[74,75] was applied to constrain covalent bond lengths, allowing an integration step of 2 fs. For the systems solvated with DMSO, all bond lengths were constrained using the SHAKE algorithm.[76,77] The reaction-field method[69,70] was applied in the calculation of electrostatic interactions. The GROMACS 4.6.1 interfaced with the PLUMED plugin package 2.0b1[78] was used. As for the free energy surfaces, the *sum hills* tool from PLUMED package was applied. Error estimates were calculated using the block-analysis technique, while the reweighting procedure was performed based on the work of Branduardi *et al.*[79]

## NOE contacts assessment in MD simulations

The complete structure of chalcones and flavonoids was submitted to microsecond MD simulations in organic solvents (chloroform or DMSO) and water. The MD conditions were generally the same of the metadynamics calculations, with longer equilibration (20 ns) and production phases (1000 ns). MD simulations were carried out by means of the GROMACS 5.0.7 package, and all the analyses employed dedicated tools from the GROMACS package, associated with in-house scripts. To allow a comparison of the simulations to H-NMR data (NOESY signals) of the compounds, nonpolar hydrogens atoms were added to frames retrieved from trajectories, using Pymol.[80] The obtained models were used to calculate the average interproton distances from simulations, using the *gmx mindist* tool from GROMACS. The average distances were computed as $\langle r^{-6} \rangle^{-1/6}$, respecting the NOE intensity for small molecules.

## Identification of conformational populations

Considering the dihedral angles of a molecule throughout a MD simulation, a conformational population is a set of conformations that share similar values for their respective dihedral angles. In order to determine these conformational populations (that is, to measure if structures share dihedral angles values close enough to be grouped together), the

following procedure was implemented: 1) The value of each dihedral angle was measured for each simulation timestep, as well as the distribution of the angle (how much of the total simulated time was spent in each angle value). These distributions were smoothed using a sliding window of length 21° using the Hann function,[81] obtaining a curve with well behaved gradient. 2) From this distribution, "peaks" and "valleys" were identified. A peak is defined as an angle with maximum local value, that is, the distribution of that angle is larger than the distribution of its immediate neighbors. Analogously, a valley is an angle with minimum local value, or angles with distribution below a given threshold that indicates a distribution value so low that the angle should be considered spurious. Knowing the peaks and valleys, dihedral populations of each torsional bond were identified by the peak angle between two valleys, corresponding to a region of high distribution. The conformational populations of a molecule were then characterized by combining the populations of each single dihedral angle (identified by the peak values) that occur at the same timestep, building a tuple of $n$ peaks, $n$ being the number of torsional bonds. Thus, all conformations identified by the same tuple of dihedral values belong to the same conformational population, the number of conformations that receive the same tuple determines the relative abundance of the conformational population, and the number of different tuples is the number of different populations throughout a simulation.

# Acknowledgement

This research received funding by the Conselho Nacional de Desenvolvimento Científico e Tecnológico (CNPq); the Coordenação de Aperfeiçoamento de Pessoal de Nível Superior (CAPES); and the Research supported by the Centro Nacional de Supercomputação of the Universidade Federal do Rio Grande do Sul (CESUP/UFRGS). This work was supported by grants from FAPERGS [16/2551-0000520-6], MCT/CNPq [311022/2015-4], CAPES-STIC AMSUD [88887.135130/2017-01] - Brazil, CAPES/Drug Discovery grant number 23038.007777/2014-

87, Alexander von Humboldt-Stiftung (AvH) [BRA 1190826 HFSTCAPES-P] - Germany.

## Supporting Information Available

The following files are available free of charge.

- Supplementary material: Conformational data regarding the sugar moieties during metadynamics calculations, Conformational data regarding the compounds on refinement MD simulations, Conformational data regarding the sugar moieties on complete compounds, inter-proton distances of the compounds simulated in water.

## References

(1) Harvey, A. L. Natural products in drug discovery. *Drug Discovery Today* **2008**, *13*, 894–901.

(2) Cragg, G. M.; Newman, D. J. Natural products: A continuing source of novel drug leads. *Biochimica et Biophysica Acta - General Subjects* **2013**, *1830*, 3670–3695.

(3) Fabricant, D. S.; Farnsworth, N. R. The value of plants used in traditional medicine for drug discovery. *Environmental health perspectives* **2001**, *109*, 69–75.

(4) Yang, Z.; Wu, W.; Wang, J.; Liu, L.; Li, L.; Yang, J.; Wang, G.; Cao, D.; Zhang, R.; Tang, M. Synthesis and biological evaluation of novel millepachine derivatives as a new class of tubulin polymerization inhibitors. *Journal of medicinal chemistry* **2014**, *57*, 7977–7989.

(5) Stoll, R.; Renner, C.; Hansen, S.; Palme, S.; Klein, C.; Belling, A.; Zeslawski, W.; Kamionka, M.; Rehm, T.; Muhlhahn, P. et al. Chalcone derivatives antagonize interactions between the human oncoprotein MDM2 and p53. *Biochemistry* **2001**, *40*, 336–344.

(6) Wang, H. M.; Zhang, L.; Liu, J.; Yang, Z. L.; Zhao, H. Y.; Yang, Y.; Shen, D.; Lu, K.; Fan, Z. C.; Yao, Q. W. et al. Synthesis and anti-cancer activity evaluation of novel prenylated and geranylated chalcone natural products and their analogs. *European Journal of Medicinal Chemistry* **2015**, *92*, 439–448.

(7) Duarte, J.; Pérez-Palencia, R.; Vargas, F.; Ocete, M. a.; Pérez-Vizcaino, F.; Zarzuelo, A.; Tamargo, J. Antihypertensive effects of the flavonoid quercetin in spontaneously hypertensive rats. *British journal of pharmacology* **2001**, *133*, 117–124.

(8) Seufi, A. M.; Ibrahim, S. S.; Elmaghraby, T. K.; Hafez, E. E. Preventive effect of the flavonoid, quercetin, on hepatic cancer in rats via oxidant/antioxidant activity: molecular and histological evidences. *Journal of experimental & clinical cancer research : CR* **2009**, *28*, 80.

(9) López, S. N.; Castelli, M. V.; Zacchino, S. a.; Domínguez, J. N.; Lobo, G.; Charris-Charris, J.; Cortés, J. C.; Ribas, J. C.; Devia, C.; Rodríguez, a. M. et al. In vitro antifungal evaluation and structure-activity relationships of a new series of chalcone derivatives and synthetic analogues, with inhibitory properties against polymers of the fungal cell wall. *Bioorganic & medicinal chemistry* **2001**, *9*, 1999–2013.

(10) Liu, H.-r.; Liu, X.-j.; Fan, H.-q.; Tang, J.-j.; Gao, X.-h.; Liu, W.-K. Design, synthesis and pharmacological evaluation of chalcone derivatives as acetylcholinesterase inhibitors. *Bioorganic & medicinal chemistry* **2014**, *22*, 6124–33.

(11) Niu, Y.; Zhu, H.; Liu, J.; Fan, H.; Sun, L.; Lu, W.; Liu, X.; Li, L. 3,5,2',4'-Tetrahydroxychalcone, a new non-purine xanthine oxidase inhibitor. *Chemico-Biological Interactions* **2011**, *189*, 161–166.

(12) Uriarte-Pueyo, I.; I Calvo, M. Flavonoids as acetylcholinesterase inhibitors. *Current medicinal chemistry* **2011**, *18*, 5289–5302.

(13) Zhuang, C.; Zhang, W.; Sheng, C.; Zhang, W.; Xing, C.; Miao, Z. Chalcone: A Privileged Structure in Medicinal Chemistry. *Chemical Reviews* **2017**, *117*, 7762–7810.

(14) Santos-Buelga, C.; Escribano-Bailon, M. T.; Lattanzio, V. *Recent Advances in Polyphenol Research*; 2010; Vol. 2; pp 1–332.

(15) Singh, P.; Anand, A.; Kumar, V. Recent developments in biological activities of chalcones: A mini review. *European Journal of Medicinal Chemistry* **2014**, *85*, 758–777.

(16) Cazarolli, L. H.; Zanatta, L.; Alberton, E. H.; Figueiredo, M. S. R. B.; Folador, P.; Damazio, R. G.; Pizzolatti, M. G.; Silva, F. R. M. B. Flavonoids: prospective drug candidates. *Mini reviews in medicinal chemistry* **2008**, *8*, 1429–1440.

(17) Jorgensen, W. L. The many roles of computation in drug discovery. *Science (New York, N.Y.)* **2004**, *303*, 1813–8.

(18) Sliwoski, G.; Kothiwale, S.; Meiler, J.; Lowe, E. W. Computational methods in drug discovery. *Pharmacological reviews* **2014**, *66*, 334–95.

(19) Durrant, J. D.; McCammon, J. A. Molecular dynamics simulations and drug discovery. *BMC biology* **2011**, *9*, 71.

(20) De Vivo, M.; Masetti, M.; Bottegoni, G.; Cavalli, A. Role of molecular dynamics and related methods in drug discovery. *Journal of medicinal chemistry* **2016**, *59*, 4035–4061.

(21) van Gunsteren, W. F.; Bakowies, D.; Baron, R.; Chandrasekhar, I.; Christen, M.; Daura, X.; Gee, P.; Geerke, D. P.; Glättli, A.; Hünenberger, P. H. et al. Biomolecular modeling: goals, problems, perspectives. *Angewandte Chemie International Edition* **2006**, *45*, 4064–4092.

(22) Cunha, R.; Soares, T.; Husu, V.; Pontes, F.; Franca, E.; Lins, R. *The Complex World of Polysaccharides*; InTech, 2012; Chapter 9, pp 229–256.

(23) Lemkul, J. A.; Allen, W. J.; Bevan, D. R. Practical considerations for building GROMOS-compatible small-molecule topologies. *Journal of Chemical Information and Modeling* **2010**, *50*, 2221–2235.

(24) Horta, B. A. C.; Merz, P. T.; Fuchs, P. F. J.; Dolenc, J.; Riniker, S.; Hünenberger, P. H. A GROMOS-Compatible Force Field for Small Organic Molecules in the Condensed Phase: The 2016H66 Parameter Set. *Journal of Chemical Theory and Computation* **2016**, *12*, 3825–3850.

(25) Polêto, M. D.; Rusu, V. H.; Grisci, B. I.; Dorn, M.; Lins, R. D.; Verli, H. Aromatic Rings Commonly Used in Medicinal Chemistry: Force Fields Comparison and Interactions With Water Toward the Design of New Chemical Entities. *Frontiers in Pharmacology* **2018**, *9*, 395.

(26) Tesch, R.; Becker, C.; Müller, M. P.; Beck, M. E.; Quambusch, L.; Getlik, M.; Lategahn, J.; Uhlenbrock, N.; Costa, F. N.; Polêto, M. D. et al. An Unusual Intramolecular Halogen Bond Guides Conformational Selection. *Angewandte Chemie International Edition 57*, 9970–9975.

(27) Oostenbrink, C.; Villa, A.; Mark, A. E.; Van Gunsteren, W. F. A biomolecular force field based on the free enthalpy of hydration and solvation: The GROMOS force-field parameter sets 53A5 and 53A6. *Journal of Computational Chemistry* **2004**, *25*, 1656–1676.

(28) Riniker, S. Fixed-Charge Atomistic Force Fields for Molecular Dynamics Simulations in the Condensed Phase: An Overview. *Journal of Chemical Information and Modeling* **2018**, *58*, 565–578.

(29) Stroet, M.; Caron, B.; Visscher, K. M.; Geerke, D. P.; Malde, A. K.; Mark, A. E. Automated Topology Builder Version 3.0: Prediction of Solvation Free Enthalpies in Water and Hexane. *Journal of Chemical Theory and Computation* **2018**, *14*, 5834–5845.

(30) Koziara, K. B.; Stroet, M.; Malde, A. K.; Mark, A. E. Testing and validation of the Automated Topology Builder (ATB) version 2.0: prediction of hydration free enthalpies. *Journal of Computer-Aided Molecular Design* **2014**, *28*, 221–233.

(31) Malde, A. K.; Zuo, L.; Breeze, M.; Stroet, M.; Poger, D.; Nair, P. C.; Oostenbrink, C.; Mark, A. E. An Automated Force Field Topology Builder (ATB) and Repository: Version 1.0. *Journal of Chemical Theory and Computation* **2011**, *7*, 4026–4037.

(32) Pedebos, C.; Pol-Fachin, L.; Verli, H. Unrestrained conformational characterization of Stenocereus eruca saponins in aqueous and nonaqueous solvents. *Journal of Natural Products* **2012**, *75*, 1196–1200.

(33) Micaelo, N. M.; Baptists, A. M.; Soares, C. M. Parametrization of 1-butyl-3-methylimidazolium hexafluorophosphate/nitrate ionic liquid for the GROMOS force field. *Journal of Physical Chemistry B* **2006**, *110*, 14444–14451.

(34) Horta, B. A. C.; Fuchs, P. F. J.; Van Gunsteren, W. F.; H??nenberger, P. H. New interaction parameters for oxygen compounds in the GROMOS force field: Improved pure-liquid and solvation properties for alcohols, ethers, aldehydes, ketones, carboxylic acids, and esters. *Journal of Chemical Theory and Computation* **2011**, *7*, 1016–1031.

(35) Caleman, C.; van Maaren, P. J.; Hong, M.; Hub, J. S.; Costa, L. T.; van der Spoel, D. Force Field Benchmark of Organic Liquids: Density, Enthalpy of Vaporization, Heat Capacities, Surface Tension, Isothermal Compressibility, Volumetric Expansion Coefficient, and Dielectric Constant. *Journal of chemical theory and computation* **2012**, *8*, 61–74.

(36) Haynes, W. *Handbook of Chemistry and Physics*; 2014; Vol. 54; p 2704.

(37) Riddick, J.; Bunger, W.; Sakano, T. Organic solvents: physical properties and methods of purification. Fourth edition. 1986.

(38) Abraham, M. H.; Whiting, G. S.; Fuchs, R.; Chambers, E. J. Thermodynamics of solute transfer from water to hexadecane. *J. Chem. Soc. Perk T 2* **1990**, *77*, 291.

(39) Chickos, J. S.; Acree, W. E. Enthalpies of vaporization of organic and organometallic compounds, 1880-2002. *Journal of Physical and Chemical Reference Data* **2003**, *32*, 519–878.

(40) Ding, F.; Peng, W.; Peng, Y.-K. Biophysical exploration of protein–flavonol recognition: effects of molecular properties and conformational flexibility. *Physical Chemistry Chemical Physics* **2016**, *18*, 11959–11971.

(41) Jo, A. R.; Kim, J. H.; Yan, X.-T.; Yang, S. Y.; Kim, Y. H. Soluble epoxide hydrolase inhibitory components from Rheum undulatum and in silico approach. *Journal of enzyme inhibition and medicinal chemistry* **2016**, *31*, 70–78.

(42) Untergehrer, M.; Bücherl, D.; Wittmann, H.-J.; Strasser, A.; Heilmann, J.; Jürgenliemk, G. Structure-Dependent Deconjugation of Flavonoid Glucuronides by Human $\beta$-Glucuronidase–In Vitro and In Silico Analyses. *Planta medica* **2015**, *81*, 1182–1189.

(43) Chinnadurai, R. K.; Saravanaraman, P.; Boopathy, R. Understanding the molecular mechanism of aryl acylamidase activity of acetylcholinesterase–An in silico study. *Archives of biochemistry and biophysics* **2015**, *580*, 1–13.

(44) Koteswara Rao, Y.; Vimalamma, G.; Venkata Rao, C.; Tzeng, Y. M. Flavonoids and andrographolides from Andrographis paniculata. *Phytochemistry* **2004**, *65*, 2317–2321.

(45) Reddy, M. K.; Reddy, M. V. B.; Reddy, B. A. K.; Gunasekar, D.; Caux, C.; Bodo, B. A New Chalcone and a Flavone from Andrographis neesiana. *Chemical and pharmaceutical bulletin* **2003**, *51*, 854–856.

(46) Nørbæk, R.; Nielsen, J. K.; Kondo, T. Flavonoids from flowers of two Crocus

chrysanthus-biflorus cultivars: 'Eye-catcher' and 'Spring Pearl' (Iridaceae). *Phytochemistry* **1999**, *51*, 1139–1146.

(47) Jayaprakasam, B.; Gunasekar, D.; Rao, K. V.; Blond, a.; Bodo, B. Androechin, A New Chalcone Glucoside from Andrographis Echioides. *Journal of Asian Natural Products Research* **2001**, *3*, 43–48.

(48) Celebre, G.; De Luca, G.; Longeri, M.; Catalano, D.; Veracini, C. A.; Emsley, J. W. Structure of biphenyl in a nematic liquid-crystalline solvent. *Journal of the Chemical Society, Faraday Transactions* **1991**, *87*, 2623.

(49) Jaime, C.; Font, J. Empirical force field calculations (MM2-V4) on biphenyl and 2,2âĂš-bipyridine. *Journal of Molecular Structure* **1989**, *195*, 103–110.

(50) Charbonnier, S.; Beguemsi, S.; N'Guessan, Y.; Legoff, D.; Proutiere, A.; Viani, R. Dihedral angle of biphenyl compounds studied by theoretical calculations (dipole induced dipole, molecular mechanics) and experimental methods (electro-optic measurements, infrared spectroscopy). *Journal of Molecular Structure* **1987**, *158*, 109–125.

(51) Huber, T.; Torda, A. E.; van Gunsteren, W. F. Local elevation: A method for improving the searching properties of molecular dynamics simulation. *Journal of Computer-Aided Molecular Design* **1994**, *8*, 695–708.

(52) Laio, A.; Parrinello, M. Escaping free-energy minima. *Proceedings of the National Academy of Sciences* **2002**, *99*, 12562–12566.

(53) Barducci, A.; Bussi, G.; Parrinello, M. Well-Tempered Metadynamics: A Smoothly Converging and Tunable Free-Energy Method. *Phys. Rev. Lett.* **2008**, *100*, 020603.

(54) Schmid, N.; Eichenberger, A. P.; Choutko, A.; Riniker, S.; Winger, M.; Mark, A. E.; van Gunsteren, W. F. Definition and testing of the GROMOS force-field versions 54A7 and 54B7. *European Biophysics Journal* **2011**, *40*, 843–856.

(55) Huang, W.; Lin, Z.; van Gunsteren, W. F. Validation of the GROMOS 54A7 Force Field with Respect to $\beta$-Peptide Folding. *Journal of Chemical Theory and Computation* **2011**, *7*, 1237–1243.

(56) Pol-Fachin, L.; Rusu, V. H.; Verli, H.; Lins, R. D. GROMOS 53A6 GLYC, an improved GROMOS force field for hexopyranose-based carbohydrates. *Journal of Chemical Theory and Computation* **2012**, *8*, 4681–4690.

(57) Frisch, M. J.; Trucks, G. W.; Schlegel, H. B.; Scuseria, G. E.; Robb, M. A.; Cheeseman, J. R.; Scalmani, G.; Barone, V.; Mennucci, B.; Petersson, G. A. et al. Gaussian 03 Revision A.01.

(58) Pol-Fachin, L.; Verli, H.; Lins, R. D. Extension and validation of the GROMOS 53A6(GLYC) parameter set for glycoproteins. *Journal of computational chemistry* **2014**, *35*, 2087–2095.

(59) Rusu, V. H.; Baron, R.; Lins, R. D. PITOMBA: Parameter Interface for Oligosaccharide Molecules Based on Atoms. *J. Chem. Theory. Comput.* **2014**, *10*, 5068–5080.

(60) Møller, C.; Plesset, M. S. Note on an Approximation Treatment for Many-Electron Systems. *Phys. Rev.* **1934**, *46*, 618–622.

(61) Mennucci, B.; Tomasi, J. Continuum solvation models: A new approach to the problem of solute's charge distribution and cavity boundaries. *The Journal of Chemical Physics* **1997**, *106*, 5151.

(62) Bayly, C.; Cieplak, P.; Cornell, W.; Kollman, P. A well-behaved electrostatic potential based method using charge restraints for deriving atomic .... *The Journal of Physical Chemistry* **1993**, 10269–10280.

(63) Van Der Spoel, D.; Lindahl, E.; Hess, B.; Groenhof, G.; Mark, A. E.; Berendsen, H. J. C. GROMACS: Fast, flexible, and free. 2005.

(64) Abraham, M. J.; Murtola, T.; Schulz, R.; P??ll, S.; Smith, J. C.; Hess, B.; Lindah, E. Gromacs: High performance molecular simulations through multi-level parallelism from laptops to supercomputers. *SoftwareX* **2015**, *1-2*, 19–25.

(65) Stark, P. B.; Parker, R. L. Bounded-variable least-squares: an algorithm and applications. *Computational Statistics* **1995**, *10*, 129–129.

(66) Branch, M. A.; Coleman, T. F.; Li, Y. A subspace, interior, and conjugate gradient method for large-scale bound-constrained minimization problems. *SIAM Journal on Scientific Computing* **1999**, *21*, 1–23.

(67) Jones, E.; Oliphant, T.; Peterson, P. SciPy: Open source scientific tools for Python. 2001–; `http://www.scipy.org/`, [Online].

(68) Berendsen, H. J. C.; Postma, J. P. M.; van Gunsteren, W. F.; DiNola, A.; Haak, J. R. Molecular dynamics with coupling to an external bath. *J. Chem. Phys.* **1984**, *81*, 3684–3690.

(69) Barker, J.; Watts, R. Monte Carlo studies of the dielectric properties of water-like models. *Molecular Physics* **1973**, *26*, 789–792.

(70) Watts, R. Monte Carlo studies of liquid water. *Molecular Physics* **1974**, *28*, 1069–1083.

(71) Van Gunsteren, W. F.; Berendsen, H. J. C. A Leap-frog Algorithm for Stochastic Dynamics. *Mol. Simulat.* **1988**, *1*, 173–185.

(72) Parrinello, M.; Rahman, A. Polymorphic transitions in single crystals: A new molecular dynamics method. *J. Appl. Phys.* **1981**, *52*, 7182.

(73) Nosé, S.; Klein, M. L. Constant pressure molecular dynamics for molecular systems. *Mol. Phys.* **1983**, *50*, 1055–1076.

(74) Hess, B.; Bekker, H.; Berendsen, H. J. C.; Fraaije, J. G. E. M. LINCS: A linear constraint solver for molecular simulations. *Journal of Computational Chemistry* **1997**, *18*, 1463–1472.

(75) Hess, B. P-LINCS: A parallel linear constraint solver for molecular simulation. *J. Chem. Theory. Comput.* **2008**, *4*, 116–122.

(76) Ryckaert, J. P.; Ciccotti, G.; Berendsen, H. J. C. Numerical integration of the cartesian equations of motion of a system with constraints: molecular dynamics of n-alkanes. *Journal of Computational Physics* **1977**, *23*, 327–341.

(77) Geerke, D. P.; van Gunsteren, W. F. Force field evaluation for biomolecular simulation: free enthalpies of solvation of polar and apolar compounds in various solvents. *ChemPhysChem* **2006**, *7*, 671–678.

(78) Tribello, G. A.; Bonomi, M.; Branduardi, D.; Camilloni, C.; Bussi, G. PLUMED 2: New feathers for an old bird. *Computer Physics Communications* **2014**, *185*, 604–613.

(79) Branduardi, D.; Bussi, G.; Parrinello, M. Metadynamics with Adaptive Gaussians. *Journal of Chemical Theory and Computation* **2012**, *8*, 2247–2254, PMID: 26588957.

(80) DeLano, W. Pymol: An open-source molecular graphics tool. *CCP4 Newsletter On Protein Crystallography* **2002**, *700*.

(81) Harris, F. J. On the use of windows for harmonic analysis with the discrete Fourier transform. *Proceedings of the IEEE* **1978**, *66*, 51–83.

# Graphical TOC Entry